

# Anisotropic upper critical field of the BiS<sub>2</sub>-based superconductor LaO<sub>0.5</sub>F<sub>0.5</sub>BiS<sub>2</sub>

Yoshikazu Mizuguchi,<sup>1,\*</sup> Atsushi Miyake,<sup>2</sup> Kazuto Akiba,<sup>2</sup> Masashi Tokunaga,<sup>2</sup> Joe Kajitani,<sup>1</sup> and Osuke Miura<sup>1</sup>

<sup>1</sup>*Department of Electrical and Electronic Engineering, Tokyo Metropolitan University, 1-1 Minami-osawa, Hachioji, Tokyo 192-0397, Japan*

<sup>2</sup>*The Institute for Solid-State Physics, University of Tokyo, 5-1-5 Kashiwanoha, Kashiwa, Chiba 277-8581, Japan*

(Received 17 April 2014; revised manuscript received 8 May 2014; published 22 May 2014)

Superconducting properties under high magnetic fields for the BiS<sub>2</sub>-based layered superconductor LaO<sub>0.5</sub>F<sub>0.5</sub>BiS<sub>2</sub> (polycrystalline sample prepared using the high-pressure synthesis method) are investigated. The anisotropy of the upper critical field is discussed by analyzing the temperature dependence of the temperature derivative of resistivity. The temperature dependence of the upper critical field shows an anomalous behavior with a characteristic magnetic field of 8 T. We reveal that the anomalous behavior is caused by the existence of three kinds of upper critical field  $\mu_0 H_{C2}^{\max}$ ,  $\mu_0 H_{C2}^{\text{mid}}$ , and  $\mu_0 H_{C2}^{\text{min}}$  in LaO<sub>0.5</sub>F<sub>0.5</sub>BiS<sub>2</sub>. The lowest upper critical field  $\mu_0 H_{C2}^{\text{min}}$  is regarded as  $\mu_0 H_{c2}$ , where the superconducting states of the grains with an orientation of  $H||c$  are suppressed. The  $\mu_0 H_{C2}^{\max}$  and  $\mu_0 H_{C2}^{\text{mid}}$  are regarded as  $\mu_0 H_{c2}$ , where the superconducting states of the grains with an orientation of  $H||ab$  are suppressed. The difference between  $\mu_0 H_{C2}^{\max}$  and  $\mu_0 H_{C2}^{\text{mid}}$  could be explained by the anisotropy of superconducting states within the Bi-S plane. The estimated anisotropy parameter of the upper critical fields is about 7.4 for the high-pressure-synthesized LaO<sub>0.5</sub>F<sub>0.5</sub>BiS<sub>2</sub> polycrystalline sample. Since this value is clearly lower than the anisotropy parameter of over 30 observed in previously reported LaO<sub>0.5</sub>F<sub>0.5</sub>BiS<sub>2</sub> single crystals grown under ambient pressure, we conclude that a larger anisotropy of superconductivity is not essential for the enhancement of  $T_c$  and lower anisotropy might be important for a higher  $T_c$  in LaO<sub>1-x</sub>F<sub>x</sub>BiS<sub>2</sub>.

DOI: [10.1103/PhysRevB.89.174515](https://doi.org/10.1103/PhysRevB.89.174515)

PACS number(s): 74.25.Dw, 74.25.Op, 74.70.Xa

## I. INTRODUCTION

Layered superconductors have drawn the attention of much research because of the appearance of unconventional superconductivity and a high transition temperature  $T_c$ . So far, two kinds of high- $T_c$  layered superconductors, cuprates and Fe-based superconductors, have been discovered [1,2]. Both of the high- $T_c$  superconductors possess a crystal structure composed of an alternate stacking of common superconducting layers and spacer layers. Recently, we discovered layered superconductors with the BiS<sub>2</sub> superconducting layers [3,4]. This family possesses a crystal structure composed of an alternate stacking of the common BiS<sub>2</sub> superconducting layers and the various spacer layers such as  $E_2O_2$  ( $E = \text{La, Ce, Pr, Nd, or Yb}$ ) [4–11],  $\text{Sr}_2\text{F}_2$  [12,13], and  $\text{Bi}_4\text{O}_4(\text{SO}_4)_{1-x}$  layers [3]. Their crystal structure at room temperature and under ambient pressure is categorized into the tetragonal space group  $P4/nmm$ . Basically, a parent phase of the BiS<sub>2</sub> family is a semiconductor with a band gap. The BiS<sub>2</sub>-based materials become metallic with electron doping into the BiS<sub>2</sub> layers and then exhibit superconductivity at low temperatures. In the superconducting phases, two Bi  $6p$  orbitals  $6p_x$  and  $6p_y$  are essential for the evolution of superconducting states [14–20].

So far, the highest  $T_c$  in the BiS<sub>2</sub>-based family is  $T_c^{\text{onset}} \sim 11$  K of LaO<sub>0.5</sub>F<sub>0.5</sub>BiS<sub>2</sub>. The superconducting properties of LaO<sub>0.5</sub>F<sub>0.5</sub>BiS<sub>2</sub> are highly sensitive to application of pressure. Although as-grown LaO<sub>0.5</sub>F<sub>0.5</sub>BiS<sub>2</sub> prepared by a solid-state reaction shows a superconducting transition with  $T_c \sim 3$  K [2], the  $T_c$  can be enhanced to over 10 K by applying high pressure [21–23]. The higher- $T_c$  phase of LaO<sub>0.5</sub>F<sub>0.5</sub>BiS<sub>2</sub> can be obtained by annealing the as-grown LaO<sub>0.5</sub>F<sub>0.5</sub>BiS<sub>2</sub> sample under a high pressure of 2 GPa. Namely, the higher- $T_c$  (high-pressure) structure could be memorized even after the sample

is put at ambient pressure after the high-pressure annealing [2,23]. One-step high-pressure synthesis can also provide a higher- $T_c$  phase of LaO<sub>0.5</sub>F<sub>0.5</sub>BiS<sub>2</sub> under the optimal synthesis conditions of 2 GPa and 700 °C [24]. Crystal structure analysis reveals that the higher- $T_c$  phase of LaO<sub>0.5</sub>F<sub>0.5</sub>BiS<sub>2</sub> can be induced by uniaxial lattice contraction along the  $c$  axis [25]. Furthermore, Tomita *et al.* reported that the lattice contraction under high pressure could be explained by a structural transition from tetragonal to monoclinic on the basis of analysis of the x-ray-diffraction patterns under high pressure and optimization of the atomic positions by using density functional theory calculations [23]. In this article, we show a largely anisotropic magnetic field-temperature  $H$ - $T$  phase diagram of superconductivity in the higher- $T_c$  phase of LaO<sub>0.5</sub>F<sub>0.5</sub>BiS<sub>2</sub>.

## II. EXPERIMENTAL DETAILS

A polycrystalline sample of LaO<sub>0.5</sub>F<sub>0.5</sub>BiS<sub>2</sub> was prepared using high-pressure synthesis with a cubic-anvil-type 180-ton press. The starting materials are the La<sub>2</sub>S<sub>3</sub> (99.9%), Bi<sub>2</sub>O<sub>3</sub> (99.99%), BiF<sub>3</sub> (99.9%), and Bi<sub>2</sub>S<sub>3</sub> powders and the Bi (99.99%) grains. The Bi<sub>2</sub>S<sub>3</sub> powder was prepared by reacting the Bi and S (99.99%) grains. The mixture with a nominal composition of LaO<sub>0.5</sub>F<sub>0.5</sub>BiS<sub>2</sub> was well mixed and pressed into a pellet. The sample was sealed into a BN crucible and inserted into a high-pressure cell composed of a carbon heater, pyrophyllite cube, and electrodes. The high-pressure cell was pressed with a pressure of 2 GPa and heated at 700 °C for 1 h.

The temperature dependence of the electrical resistivity  $\rho$ - $T$  was measured using a four-terminal method under magnetic fields up to 14 T with a Physical Property Measurement System (Quantum Design). The magnetic field dependence of the electrical resistivity  $\rho$ - $H$  in pulsed magnetic fields up to  $\sim 56$  T was measured by utilizing a nondestructive pulsed magnet at the Institute for Solid State Physics (University

\*mizugu@tmu.ac.jp

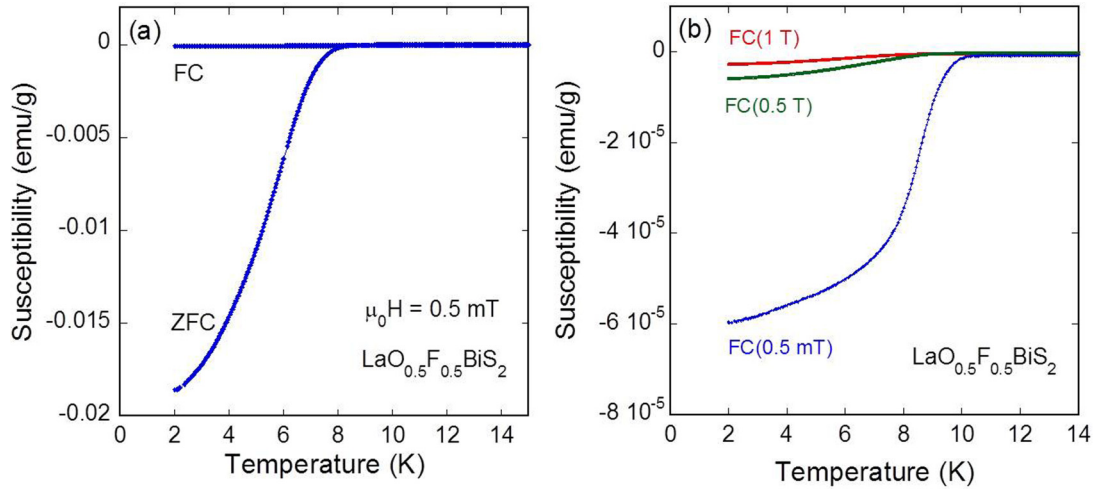


FIG. 1. (Color online) (a) Temperature dependence of magnetic susceptibility for the polycrystalline sample of  $\text{LaO}_{0.5}\text{F}_{0.5}\text{BiS}_2$  prepared using the high-pressure-synthesis method. (b) Temperature dependence of FC susceptibility for  $\text{LaO}_{0.5}\text{F}_{0.5}\text{BiS}_2$  with applied fields of 0.5 mT, 0.5 T, and 1 T.

of Tokyo) using the four-terminal method. The duration of the pulsed magnetic field was about 36 ms. In the electrical resistivity measurements, the direction of current was parallel to the applied magnetic fields. The temperature dependence of the magnetic susceptibility after both zero-field cooling (ZFC) and field cooling (FC) was measured using a superconducting interference device magnetometer (MPMS3, Quantum Design) with applied magnetic fields up to 3 T.

### III. RESULTS AND DISCUSSION

Figure 1(a) shows the temperature dependence of the magnetic susceptibility for  $\text{LaO}_{0.5}\text{F}_{0.5}\text{BiS}_2$  under a field of 0.5 mT. Below 11 K, diamagnetic signals corresponding to the evolution of superconducting states are observed. The irreversible temperature  $T_c^{\text{irr}}$ , which is a bifurcation point between the ZFC and FC curves, is 8.5 K. Figure 1(b)

displays the temperature dependence of the FC susceptibility for  $\text{LaO}_{0.5}\text{F}_{0.5}\text{BiS}_2$  with applied fields of 0.5 mT, 0.5 T, and 1 T. It is found that the superconducting states can be destroyed by applying a relatively small field of 1 T. At the same time, we clearly note that the onset of  $T_c$  is robust against the application of high magnetic fields.

Figure 2(a) shows the temperature dependence of electrical resistivity for  $\text{LaO}_{0.5}\text{F}_{0.5}\text{BiS}_2$  under magnetic fields up to 14 T. The  $T_c^{\text{onset}}$  and  $T_c^{\text{zero}}$  under 0 T are 10.8 and 7.7 K, respectively. Here we define  $T_c^{\text{onset}}$  as the temperature at which resistivity begins to decrease in the  $\rho$ - $T$  measurements. Figure 2(b) shows the enlargement of the temperature dependence of the resistivity near  $T_c^{\text{onset}}$ . With increasing magnetic field,  $T_c^{\text{zero}}$  is largely suppressed and the zero-resistivity state is not observed above 3 T within a temperature range  $T > 2$  K. In contrast, the kink observed at  $T_c^{\text{onset}}$  under 0 T is robust against the application of high magnetic fields and still observable at

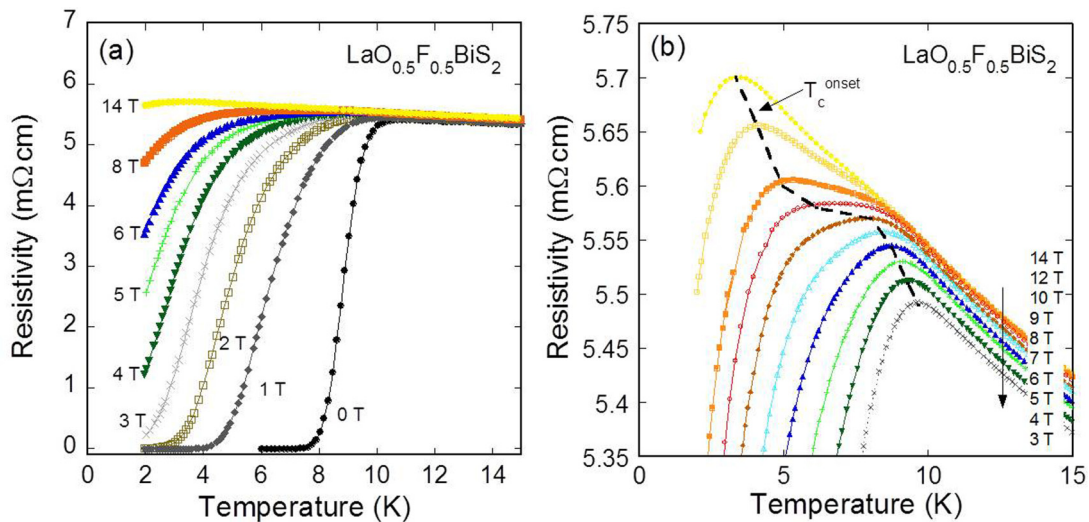


FIG. 2. (Color online) (a) Temperature dependence of electrical resistivity for  $\text{LaO}_{0.5}\text{F}_{0.5}\text{BiS}_2$  under magnetic fields up to 14 T. (b) Enlargement of the temperature dependence of electrical resistivity for  $\text{LaO}_{0.5}\text{F}_{0.5}\text{BiS}_2$  under magnetic fields up to 14 T. The dashed line indicates  $T_c^{\text{onset}}$ .

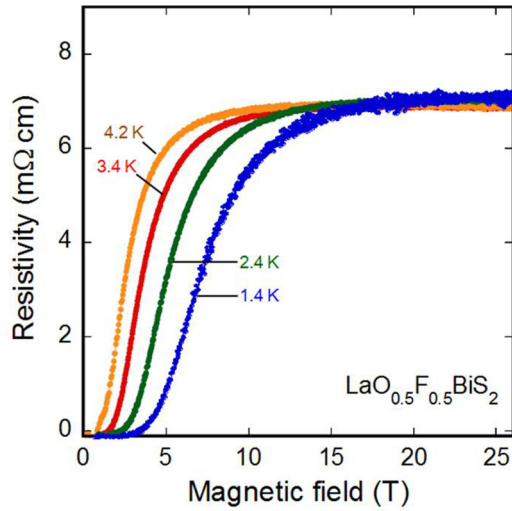


FIG. 3. (Color online) Magnetic field dependence of electrical resistivity for  $\text{LaO}_{0.5}\text{F}_{0.5}\text{BiS}_2$  at temperatures of 1.4, 2.4, 3.4, and 4.2 K.

14 T. As will be discussed later, the  $\rho(T)$  curves above 6 T show an additional anomaly [see Fig. 2(b)]. To obtain further information under higher magnetic fields, we performed the  $\rho$ - $H$  measurements in pulsed magnetic fields up to 56 T. Figure 3 shows the field dependence of the electrical resistivity at 1.4, 2.4, 3.4, and 4.2 K. The onset point  $\mu_0 H_{c2}$  (pulse) of the superconducting transition is estimated using a criterion of 99% of the normal state resistivity. Above  $\mu_0 H_{c2}$ , the resistivity is almost constant as a function of fields. The  $\mu_0 H_{c2}$  is estimated to be 18.7, 15.4, 12.7, and 10.7 T for 1.4, 2.4, 3.4, and 4.2 K, respectively.

To analyze the obtained data of the resistivity under various magnetic fields, we plotted the  $\mu_0 H_{c2}$  and  $\mu_0 H_{irr}$  estimated using  $T_c^{\text{onset}}$  and  $T_c^{\text{zero}}$  in the  $\rho$ - $T$  measurements in Fig. 4. The  $\mu_0 H_{c2}$  estimated from the  $\rho$ - $H$  measurements with pulsed magnetic fields is also plotted in Fig. 4. The  $\mu_0 H_{c2}$  (pulse) agrees with the  $H_{c2}$  ( $\rho$ - $T$ ). It is found that

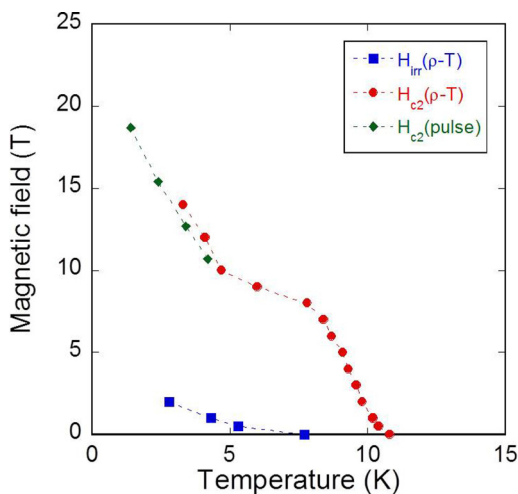


FIG. 4. (Color online) Temperature dependence of  $\mu_0 H_{c2}$  ( $\rho$ - $T$ ),  $\mu_0 H_{irr}$  ( $\rho$ - $T$ ), and  $\mu_0 H_{c2}$  (pulse).

$\mu_0 H_{irr}$  is much lower than  $\mu_0 H_{c2}$ . This can be understood by the large anisotropy of superconductivity in the  $\text{BiS}_2$ -based superconductors. Recently, Nagao *et al.* reported that the anisotropy of superconductivity in  $\text{EO}_{1-x}\text{F}_x\text{BiS}_2$  was quite large and was relevant to those of cuprate superconductors [26,27]. The sample used in this study is polycrystalline; hence, the grain orientation should be random. Generally, in the layered superconductors with large anisotropy of superconductivity, the superconducting states in the grains whose  $c$  axis is parallel to the applied magnetic fields are strongly suppressed by applying high magnetic fields. It is conceivable that the large suppression of the fraction of the FC susceptibility at high magnetic fields is caused by the large anisotropy of superconductivity in  $\text{LaO}_{0.5}\text{F}_{0.5}\text{BiS}_2$ . In other words, the superconducting states for some grains are suppressed by applying magnetic fields.

As shown in Fig. 4, the temperature dependence of  $\mu_0 H_{c2}$  shows an anomalous curve with a characteristic field of  $\sim 8$  T. To clarify the anomalous behavior of  $\mu_0 H_{c2}$ , we analyzed the anisotropy of  $\mu_0 H_{c2}$  using the method proposed by Bud'ko *et al.* [28]. They showed that the anisotropy of  $\mu_0 H_{c2}$  for the randomly oriented powder samples of layered superconductors could be estimated by analyzing the temperature dependence of the temperature derivative of magnetization  $dM/dT$ . In the method, the maximum upper critical field  $\mu_0 H_{c2}^{\text{max}}$ , which could be regarded as the  $H_{c2}$  for the grains with a grain orientation of  $H \parallel ab$ , can be estimated from the onset of  $dM/dT$ ; we call the onset temperature  $T^{\text{max}}$ . The minimum upper critical field  $H_{c2}^{\text{min}}$ , which can be regarded as the  $\mu_0 H_{c2}$  for the grains with  $H \parallel c$ , can be estimated from the kink in the  $dM/dT$ - $T$  curve; we call this temperature  $T^{\text{min}}$ . Since the analysis proposed in Ref. [28] relies on the fact that the polycrystalline sample under study is a single phase, we should mention that the present polycrystalline sample was characterized as a single phase except for tiny impurities of  $\text{Bi}_2\text{S}_3$  by powder x-ray diffraction [25].

The temperature dependence of  $dM/dT$  for  $\text{LaO}_{0.5}\text{F}_{0.5}\text{BiS}_2$  under various magnetic fields of 0.5, 1, 2, and 3 T is shown in Figs. 5(a)–5(d), respectively. As represented in Fig. 5(b), we clearly observe  $T^{\text{max}}$  and  $T^{\text{min}}$  as observed in the  $\text{MgB}_2$  and  $\text{LuNi}_2\text{B}_2\text{C}$  superconductors [28]. However, the signal-to-noise (S/N) ratio becomes smaller at high magnetic fields due to the large suppression of bulk characteristics of superconductivity. Therefore, we discuss  $\mu_0 H_{c2}^{\text{max}}$  and  $\mu_0 H_{c2}^{\text{min}}$  by analyzing the temperature derivative of the electrical resistivity to clarify the anomalous behavior of the  $\mu_0 H_{c2}$ - $T$  curve under high magnetic fields. As shown in Figs. 5(a)–5(d), it was confirmed that the  $T^{\text{max}}$  and  $T^{\text{min}}$  estimated using the  $dM/dT$ - $T$  curve almost correspond to those estimated using the  $d\rho/dT$ - $T$  curve under all magnetic fields up to 3 T. Furthermore, the S/N ratio of the  $d\rho/dT$ - $T$  curve is clearly better than that of the  $dM/dT$ - $T$  curve. Therefore, we here investigate the anisotropy of  $\mu_0 H_{c2}$  by analyzing the  $d\rho/dT$ - $T$  data.

As shown in Figs. 5(a)–5(d), both  $T^{\text{max}}$  and  $T^{\text{min}}$  shift to lower temperatures with increasing magnetic field. In particular,  $T^{\text{min}}$  is rapidly suppressed with increasing field and becomes below 2 K above 4 T. Therefore,  $\mu_0 H_{c2}^{\text{min}}$  (0 K) is expected to be less than 5 T. At above 5 T, we observed an additional inflection point in the  $d\rho/dT$ - $T$  curves. Figure 6(a) shows the  $d\rho/dT$ - $T$  and  $\rho$ - $T$  curves for  $\text{LaO}_{0.5}\text{F}_{0.5}\text{BiS}_2$  under

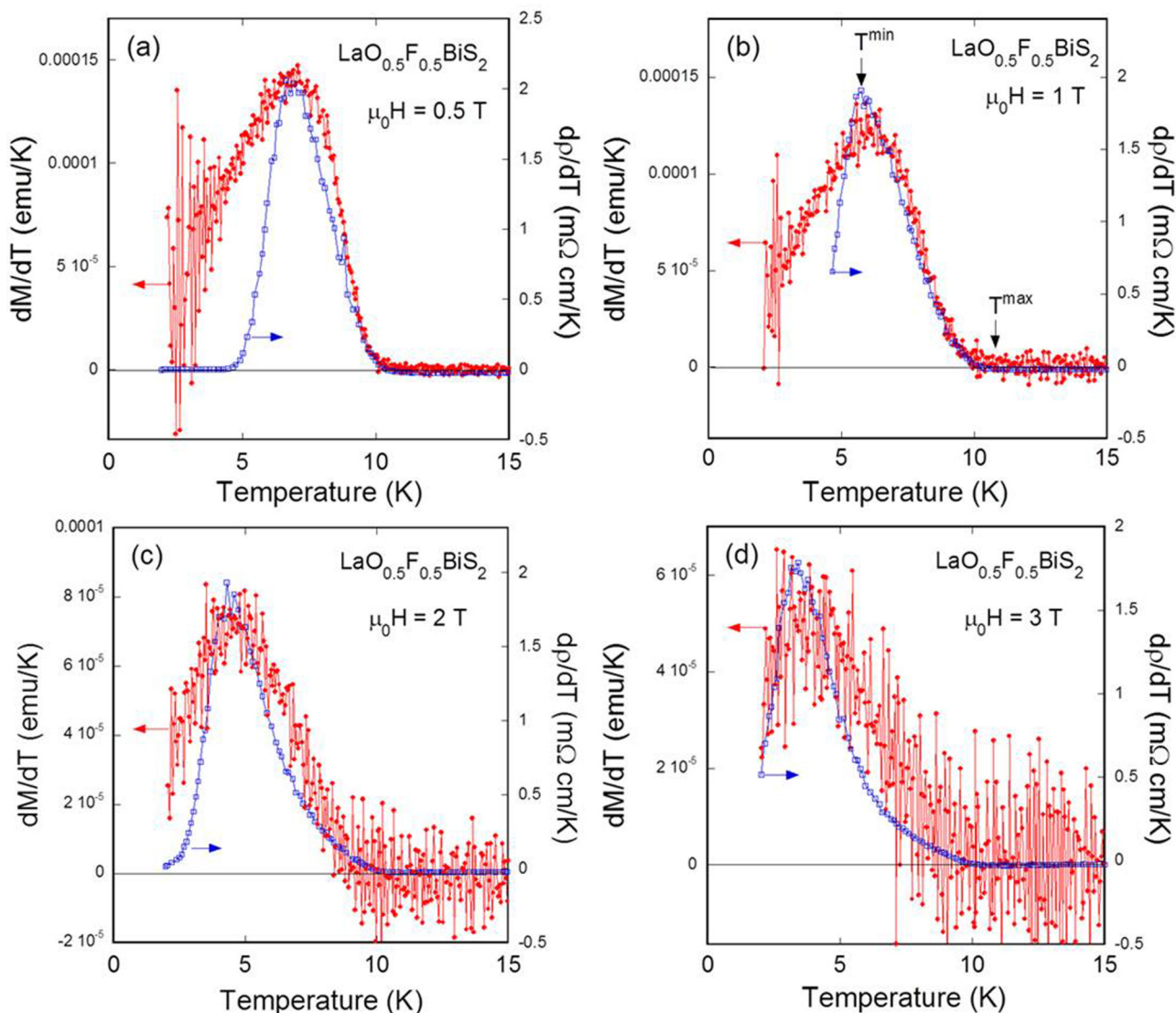


FIG. 5. (Color online) Temperature dependence of  $dM/dT$  and  $d\rho/dT$  for  $\text{LaO}_{0.5}\text{F}_{0.5}\text{BiS}_2$  under applied magnetic fields of (a) 0.5 T, (b) 1 T, (c) 2 T, and (d) 3 T. In (b), the  $T^{\text{max}}$  and  $T^{\text{min}}$  are indicated with arrows.

a magnetic field of 8 T. The onset point  $T^{\text{max}}$  is still above 9 K. The  $T_c^{\text{onset}}(\rho-T)$  corresponds to the temperature at which the value of the  $d\rho/dT$  equals zero. The inflection point appears at  $\sim 5.3$  K; here we call this characteristic temperature  $T^{\text{mid}}$ . Below  $T^{\text{mid}}$ , the value of  $d\rho/dT$  begins to increase rapidly. At the same time, the resistivity begins to decrease largely, which indicates the evolution of the superconducting current path below  $T^{\text{mid}}$ . Figure 6(b) displays the increase of the temperature dependence of the resistivity under various magnetic fields up to 14 T. The  $T^{\text{mid}}$  estimated from the  $d\rho/dT-T$  curves using the same method as in Fig. 6(a) is indicated by arrows in Fig. 6(b). With increasing magnetic fields, the anomaly at  $T^{\text{mid}}$  on the  $\rho-T$  curve is more pronounced. Then  $T^{\text{mid}}$  overlaps with  $T_c^{\text{onset}}$  under magnetic fields above 10 T. It can be considered that  $T_c^{\text{onset}}$ , which denotes the evolution of the superconducting current path, corresponds to  $T^{\text{max}}$  under lower magnetic fields, while it corresponds to  $T^{\text{mid}}$  under higher magnetic fields, hence the anomalous behavior of the  $\mu_0 H_{c2}-T$  curve shown in Fig. 4.

In Fig. 7(a) we have plotted  $\mu_0 H_{c2}^{\text{max}}(T)$ ,  $\mu_0 H_{c2}^{\text{mid}}(T)$ , and  $\mu_0 H_{c2}^{\text{min}}(T)$  with the data points of  $\mu_0 H_{c2}(\rho-T)$ ,  $\mu_0 H_{\text{irr}}(\rho-T)$ , and  $\mu_0 H_{c2}$  (pulse). The  $\mu_0 H_{c2}^{\text{min}}(T)$  is obviously lower than  $\mu_0 H_{c2}^{\text{max}}$  and  $\mu_0 H_{c2}^{\text{mid}}$  at whole temperatures and is located near  $H_{\text{irr}}(T)$ . As mentioned above, the low  $\mu_0 H_{c2}^{\text{min}}$  can be understood by the large anisotropy of superconductivity of  $\text{LaO}_{0.5}\text{F}_{0.5}\text{BiS}_2$ . Namely, the superconducting current path can be easily destroyed under magnetic fields for the grains with a grain orientation of  $H\parallel c$ . Next we discuss the difference between  $\mu_0 H_{c2}^{\text{max}}$  and  $\mu_0 H_{c2}^{\text{mid}}$ . As shown in Fig. 7(a), the temperature dependence curve of  $\mu_0 H_{c2}(\rho-T)$  almost overlaps with the  $\mu_0 H_{c2}^{\text{max}}(T)$  curve under magnetic fields up to 5 T. Then it deviates from the  $\mu_0 H_{c2}^{\text{max}}(T)$  curve. Interestingly, the curve of the temperature dependence of  $\mu_0 H_{c2}(\rho-T)$  finally overlaps with the  $\mu_0 H_{c2}^{\text{mid}}(T)$  curve under magnetic fields above 10 T. The observed anomalous behavior of the  $\mu_0 H_{c2}-T$  curve implies that the superconducting current path is generated below  $T^{\text{max}}$  under lower magnetic fields, while it is generated below  $T^{\text{mid}}$  under higher magnetic fields. Therefore,

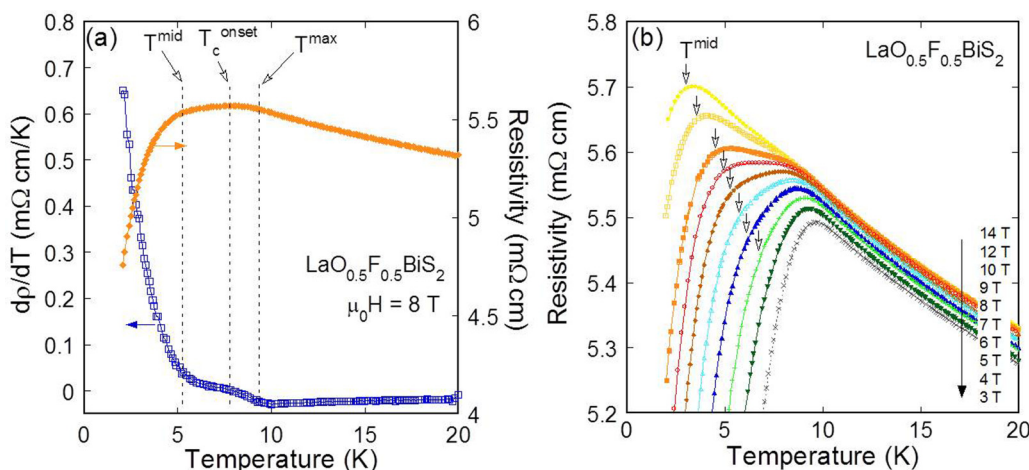


FIG. 6. (Color online) (a) Temperature dependence of resistivity  $\rho$  and  $d\rho/dT$  for  $\text{LaO}_{0.5}\text{F}_{0.5}\text{BiS}_2$  under a magnetic field of 8 T. The  $T^{\text{mid}}$  and  $T^{\text{max}}$  are indicated with dashed lines and arrows. The  $T_c^{\text{onset}}$  is the temperature where resistivity begins to decrease. (b) Enlargement of the temperature dependence of electrical resistivity for  $\text{LaO}_{0.5}\text{F}_{0.5}\text{BiS}_2$  under magnetic fields up to 14 T. The  $T^{\text{mid}}$  is indicated with arrows.

there should be a factor that affects upper critical field, except for the difference in the grain orientation between  $H\parallel ab$  and  $H\parallel c$ .

To explain the difference between the two kinds of upper critical field  $\mu_0 H_{c2}^{\text{max}}$  and  $\mu_0 H_{c2}^{\text{mid}}$ , we assume that the superconducting states within the  $ab$  plane are anisotropic. The structure distortion (or strain) could exist in the present sample of  $\text{LaO}_{0.5}\text{F}_{0.5}\text{BiS}_2$  prepared using the high-pressure-synthesis technique, as observed in the previous high-pressure studies on superconductivity and the crystal structure of  $\text{LaO}_{0.5}\text{F}_{0.5}\text{BiS}_2$  [23]. Although the evidence of the lowering of the symmetry of the crystal structure was not detected in the x-ray-diffraction measurements, the broadening of the  $(h00)$  and  $(00l)$  peaks was observed in the high-pressure  $\text{LaO}_{0.5}\text{F}_{0.5}\text{BiS}_2$  samples [25,29]. Therefore, it is conceivable that the crystal structure of the present  $\text{LaO}_{0.5}\text{F}_{0.5}\text{BiS}_2$  polycrystalline sample is not a perfect tetragonal structure. If the  $ab$  plane is distorted (or

strained), the superconducting states along the  $a$  axis could be nonequivalent to that along the  $b$  axis. In that case, the upper critical field for the  $a$ -axis direction and the  $b$ -axis direction could be different due to the difference in effective mass. In addition, a previous theoretical study suggested that the one-dimensional nature of the Bi bands (Bi  $6p_x$  and Bi  $6p_y$ ) provides good nesting of the Fermi surface in the  $\text{LaO}_{1-x}\text{F}_x\text{BiS}_2$  system [14]. Furthermore, Suzuki *et al.* showed that the band structure of the  $\text{BiS}_2$  family could be largely affected by the change in the local crystal structures [15]. These theoretical studies could suggest the possibility of the appearance of the anisotropic superconducting states within the  $ab$  plane when the degeneracy of Bi  $6p_x$  and Bi  $6p_y$  is lifted. Therefore, it is conceivable that there are the different upper critical fields  $\mu_0 H_{c2}^{a\text{ axis}}$  and  $\mu_0 H_{c2}^{b\text{ axis}}$  in a distorted (or strained) Bi-S plane of  $\text{LaO}_{0.5}\text{F}_{0.5}\text{BiS}_2$ . On the basis of the discussion, the evolution of the anisotropic superconducting

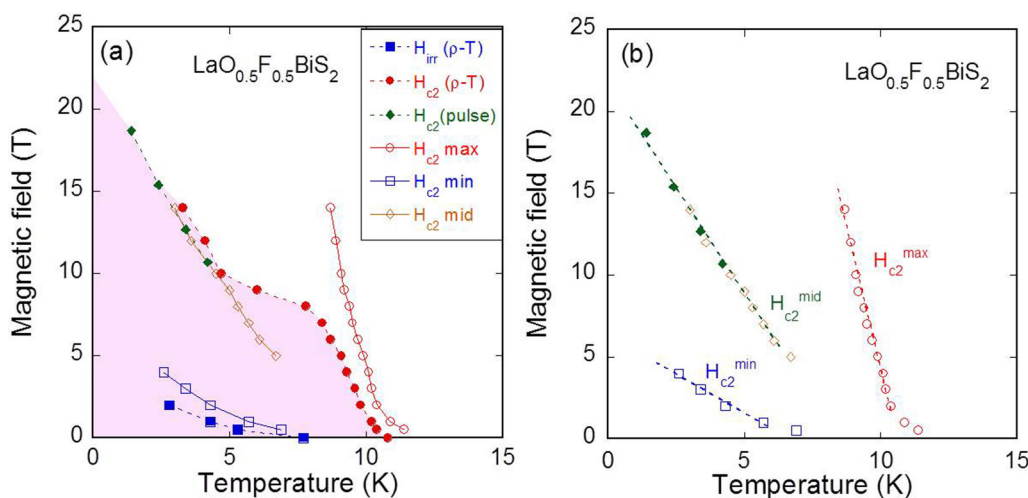


FIG. 7. (Color online) (a) Magnetic field–temperature phase diagram of  $\text{LaO}_{0.5}\text{F}_{0.5}\text{BiS}_2$  established with the estimated  $\mu_0 H_{c2}$  (pulse),  $\mu_0 H_{c2}^{\text{max}}$ ,  $\mu_0 H_{c2}^{\text{mid}}$ , and  $\mu_0 H_{c2}^{\text{min}}$ . The  $\mu_0 H_{c2}(\rho-T)$  and  $\mu_0 H_{\text{irr}}(\rho-T)$  are also plotted. In the colored area, below  $T_c^{\text{onset}}(\rho-T)$ , the path of the superconducting current is generated. (b) Magnetic field–temperature phase diagram of  $\text{LaO}_{0.5}\text{F}_{0.5}\text{BiS}_2$  with three kinds of upper critical fields  $\mu_0 H_{c2}^{\text{max}}$ ,  $\mu_0 H_{c2}^{\text{mid}}$ , and  $\mu_0 H_{c2}^{\text{min}}$ . The dashed lines are the linear fitting lines for  $\mu_0 H_{c2}^{\text{max}}$ ,  $\mu_0 H_{c2}^{\text{mid}}$ , and  $\mu_0 H_{c2}^{\text{min}}$ .

states of  $\text{LaO}_{0.5}\text{F}_{0.5}\text{BiS}_2$  under magnetic fields is summarized below. All the grains are superconducting at  $\mu_0 H < \mu_0 H_{C2}^{\min}$ . At magnetic fields of  $\mu_0 H_{C2}^{\min} < \mu_0 H < \mu_0 H_{C2}^{\text{mid}}$ , superconducting states of the grains with a grain orientation of  $H \parallel c$  are suppressed. Then, under  $\mu_0 H_{C2}^{\text{mid}} < \mu_0 H < \mu_0 H_{C2}^{\text{max}}$ , the superconducting states of the grains with an orientation of  $H \parallel a$  or  $H \parallel b$  are suppressed; we cannot distinguish the  $a$ -axis orientation from the  $b$ -axis orientation within the results of the present study. Above  $\mu_0 H_{C2}^{\text{max}}$ , all the grains become nonsuperconducting.

To discuss the anisotropy of the upper critical field, we have plotted the values of  $\mu_0 H_{C2}^{\text{max}}(T)$ ,  $\mu_0 H_{C2}^{\text{mid}}(T)$ , and  $\mu_0 H_{C2}^{\min}(T)$  in Fig. 7(b). The data points for  $\mu_0 H_{C2}^{\text{mid}}$  and  $\mu_0 H_{C2}$  (pulse) exhibit a linear temperature dependence. Therefore, we estimated  $d\mu_0 H_{C2}^{\text{max}}/dT$ ,  $d\mu_0 H_{C2}^{\text{mid}}/dT$ , and  $d\mu_0 H_{C2}^{\min}/dT$  by fitting the data points with a linear function of temperature to discuss the anisotropy. The estimated  $d\mu_0 H_{C2}^{\text{max}}/dT$ ,  $d\mu_0 H_{C2}^{\text{mid}}/dT$ , and  $d\mu_0 H_{C2}^{\min}/dT$  are  $-7.05$ ,  $-2.60$ , and  $-0.95$  T/K, respectively. The anisotropy parameter estimated using the values of  $d\mu_0 H_{C2}^{\text{max}}/dT$  and  $d\mu_0 H_{C2}^{\min}/dT$  is 7.4. The anisotropy parameter estimated in this work is clearly lower than the anisotropy parameter of over 30 for  $\text{LaO}_{1-x}\text{F}_x\text{BiS}_2$  single crystals ( $T_c \sim 3$  K) grown at ambient pressure [27]. This indicates that the larger anisotropy of superconductivity is not essential for the enhancement of  $T_c$  and the lower anisotropy may be important for a higher  $T_c$  in  $\text{LaO}_{1-x}\text{F}_x\text{BiS}_2$ . Furthermore, the evolution of the in-plane anisotropy within Bi-S plane may play an important role in the enhancement of  $T_c$ . To elucidate the mechanism of superconductivity in the  $\text{BiS}_2$  family, high-field studies using  $\text{LaO}_{1-x}\text{F}_x\text{BiS}_2$  single crystals with higher  $T_c$  are needed. To achieve this, single crystal growth of the high- $T_c$  phase of  $\text{LaO}_{1-x}\text{F}_x\text{BiS}_2$  is required.

#### IV. CONCLUSION

We have studied magnetic and transport properties of the high-pressure-synthesized  $\text{LaO}_{0.5}\text{F}_{0.5}\text{BiS}_2$  polycrystalline sample under high magnetic fields. The temperature

dependence of the upper critical field shows anomalous behavior with a characteristic magnetic field of 8 T. We found that the anisotropy of the upper critical field of the polycrystalline sample of  $\text{LaO}_{0.5}\text{F}_{0.5}\text{BiS}_2$  can be estimated by analyzing the characteristic temperatures on the  $d\rho/dT$ - $T$  curve. It was found that there were three kinds of upper critical field in  $\text{LaO}_{0.5}\text{F}_{0.5}\text{BiS}_2$ . The lowest upper critical field  $\mu_0 H_{C2}^{\min}$  is regarded as  $\mu_0 H_{c2}$  when the magnetic fields are applied parallel to the  $c$  axis of the grain. The  $\mu_0 H_{C2}^{\text{max}}$  and  $\mu_0 H_{C2}^{\text{mid}}$  are regarded as  $\mu_0 H_{c2}$  when the superconducting states are suppressed for the grains with an orientation of  $H \parallel ab$ . The difference between  $\mu_0 H_{C2}^{\text{max}}$  and  $\mu_0 H_{C2}^{\text{mid}}$  could be explained by the anisotropy of superconducting states within the Bi-S plane, which is possibly caused by the lattice distortion or strain within the Bi-S plane. Hence, the upper critical fields  $\mu_0 H_{C2}^{a \text{ axis}}$  and  $\mu_0 H_{C2}^{b \text{ axis}}$  are different due to the difference in the effective mass. The fraction of grains in superconducting states decreases with increasing magnetic field on the order of 0 T,  $\mu_0 H_{C2}^{\min}$ ,  $\mu_0 H_{C2}^{\text{mid}}$ , and  $\mu_0 H_{C2}^{\text{max}}$ . Above  $\mu_0 H_{C2}^{\text{max}}$ , all the grains become nonsuperconducting. The estimated  $d\mu_0 H_{C2}^{\text{max}}/dT$ ,  $d\mu_0 H_{C2}^{\text{mid}}/dT$ , and  $d\mu_0 H_{C2}^{\min}/dT$  are  $-7.05$ ,  $-2.60$ , and  $-0.95$  T/K, respectively. The anisotropy parameter for the upper critical field estimated using  $d\mu_0 H_{C2}^{\text{max}}/dT$  and  $d\mu_0 H_{C2}^{\min}/dT$  is 7.4, which is clearly lower than the anisotropy parameter of over 30 in the previous report for  $\text{LaO}_{1-x}\text{F}_x\text{BiS}_2$  single crystals ( $T_c \sim 3$  K) grown at ambient pressure. This indicates that the larger anisotropy of superconductivity is not essential for the enhancement of  $T_c$  and the lower anisotropy might be important for a higher  $T_c$  in  $\text{LaO}_{1-x}\text{F}_x\text{BiS}_2$ . Moreover, the evolution of the in-plane anisotropy within the Bi-S plane may play an important role for the enhancement of  $T_c$  in  $\text{LaO}_{1-x}\text{F}_x\text{BiS}_2$ .

#### ACKNOWLEDGMENTS

The authors would like to thank K. Kuroki of Osaka University for fruitful discussion. This work was partly supported by JSPS KAKENHI Grants No. 25707031 and No. 23340096.

- 
- [1] J. G. Bednorz and K. A. Müller, *Z. Phys. B* **64**, 189 (1986).
  - [2] Y. Kamihara, T. Watanabe, M. Hirano, and H. Hosono, *J. Am. Chem. Soc.* **130**, 3296 (2008).
  - [3] Y. Mizuguchi, H. Fujihisa, Y. Gotoh, K. Suzuki, H. Usui, K. Kuroki, S. Demura, Y. Takano, H. Izawa, and O. Miura, *Phys. Rev. B* **86**, 220510 (2012).
  - [4] Y. Mizuguchi, S. Demura, K. Deguchi, Y. Takano, H. Fujihisa, Y. Gotoh, H. Izawa, and O. Miura, *J. Phys. Soc. Jpn.* **81**, 114725 (2012).
  - [5] J. Xing, S. Li, X. Ding, H. Yang, and H. H. Wen, *Phys. Rev. B* **86**, 214518 (2012).
  - [6] S. Demura, K. Deguchi, Y. Mizuguchi, K. Sato, R. Honjyo, A. Yamashita, T. Yamaki, H. Hara, T. Watanabe, S. J. Denholme, M. Fujioka, H. Okazaki, T. Ozaki, O. Miura, T. Yamaguchi, H. Takeya, and Y. Takano, [arXiv:1311.4267](https://arxiv.org/abs/1311.4267).
  - [7] R. Jha, A. Kumar, S. K. Singh, and V. P. S. Awana, *J. Supercond. Novel Magn.* **26**, 499 (2013).
  - [8] J. Kajitani, K. Deguchi, T. Hiroi, A. Omachi, S. Demura, Y. Takano, O. Miura, and Y. Mizuguchi, *J. Phys. Soc. Jpn.* **83**, 065002 (2014).
  - [9] S. Demura, Y. Mizuguchi, K. Deguchi, H. Okazaki, H. Hara, T. Watanabe, S. J. Denholme, M. Fujioka, T. Ozaki, H. Fujihisa, Y. Gotoh, O. Miura, T. Yamaguchi, H. Takeya, and Y. Takano, *J. Phys. Soc. Jpn.* **82**, 033708 (2013).
  - [10] R. Jha, A. Kumar, S. K. Singh, and V. P. S. Awana, *J. Appl. Phys.* **113**, 056102 (2013).
  - [11] D. Yazici, K. Huang, B. D. White, A. H. Chang, A. J. Friedman, and M. B. Maple, *Philos. Mag.* **93**, 673 (2012).
  - [12] X. Lin, X. Ni, B. Chen, X. Xu, X. Yang, J. Dai, Y. Li, X. Yang, Y. Luo, Q. Tao, G. Cao, and Z. Xu, *Phys. Rev. B* **87**, 020504 (2013).
  - [13] H. Sakai, D. Kotajima, K. Saito, H. Wadati, Y. Wakisaka, M. Mizumaki, K. Nitta, Y. Tokura, and S. Ishiwata, *J. Phys. Soc. Jpn.* **83**, 014709 (2014).

- [14] H. Usui, K. Suzuki, and K. Kuroki, *Phys. Rev. B* **86**, 220501 (2012).
- [15] K. Suzuki, H. Usui, and K. Kuroki, *Phys. Procedia* **45**, 21 (2013).
- [16] T. Yildirim, *Phys. Rev. B* **87**, 020506(R) (2013).
- [17] I. R. Shein and A. L. Ivanovskii, *JETP Lett.* **96**, 769 (2012).
- [18] B. Li, Z. W. Xing, and G. Q. Huang, *Europhys. Lett.* **101**, 47002 (2013).
- [19] G. B. Martins, A. Moreo, and E. Dagotto, *Phys. Rev. B* **87**, 081102(R) (2013).
- [20] C. Morice, E. Artacho, S. E. Dutton, D. Molnar, H. J. Kim, and S. S. Saxena, [arXiv:1312.2615](https://arxiv.org/abs/1312.2615).
- [21] H. Kotegawa, Y. Tomita, H. Tou, H. Izawa, Y. Mizuguchi, O. Miura, S. Demura, K. Deguchi, and Y. Takano, *J. Phys. Soc. Jpn.* **81**, 103702 (2012).
- [22] C. T. Wolowiec, B. D. White, I. Jeon, D. Yazici, K. Huang, and M. B. Maple, *J. Phys.: Condens. Matter* **25**, 422201 (2013).
- [23] T. Tomita, M. Ebata, H. Soeda, H. Takahashi, H. Fujihisa, Y. Gotoh, Y. Mizuguchi, H. Izawa, O. Miura, S. Demura, K. Deguchi, and Y. Takano, [arXiv:1309.4250](https://arxiv.org/abs/1309.4250) [*J. Phys. Soc. Jpn.* (to be published)].
- [24] K. Deguchi, Y. Mizuguchi, S. Demura, H. Hara, T. Watanabe, S. J. Denholme, M. Fujioka, H. Okazaki, T. Ozaki, H. Takeya, T. Yamaguchi, O. Miura, and Y. Takano, *Europhys. Lett.* **101**, 17004 (2013).
- [25] Y. Mizuguchi, T. Hiroi, J. Kajitani, H. Takatsu, H. Kadowaki, and O. Miura, *J. Phys. Soc. Jpn.* **83**, 053704 (2014).
- [26] M. Nagao, S. Demura, K. Deguchi, A. Miura, S. Watauchi, T. Takei, Y. Takano, N. Kumada, and I. Tanaka, *J. Phys. Soc. Jpn.* **82**, 113701 (2013).
- [27] M. Nagao, A. Miura, S. Demura, K. Deguchi, S. Watauchi, T. Takei, Y. Takano, N. Kumada, and I. Tanaka, *Solid State Commun.* **178**, 33 (2014).
- [28] S. L. Bud'ko, V. G. Kogan, and P. C. Canfield, *Phys. Rev. B* **64**, 180506 (2001).
- [29] J. Kajitani, K. Deguchi, A. Omachi, T. Hiroi, Y. Takano, H. Takatsu, H. Kadowaki, O. Miura, and Y. Mizuguchi, *Solid State Commun.* **181**, 1 (2014).